Characteristics of transport in electron internal transport barriers and in the vicinity of rational surfaces in the Large Helical Device[a]

K. Ida,[1,b] S. Inagaki,[1] T. Shimozuma,[1] N. Tamura,[1] H. Funaba,[1] K. Narihara,[1] S. Kubo,[1]
S. Murakami,[2] A. Wakasa,[3] M. Yokoyama,[1] Y. Takeiri,[1] K. Y. Watanabe,[1] K. Tanaka,[1]
M. Yoshinuma,[1] Y. Liang,[4] N. Ohyabu,[1] T. Akiyama,[1] N. Ashikawa,[1] M. Emoto,[1] T. Fujita,[5]
T. Fukuda,[6] P. Goncharov,[7] M. Goto,[1] H. Idei,[8] K. Ikeda,[1] A. Isayama,[5] M. Isobe,[1]
O. Kaneko,[1] K. Kawahata,[1] H. Kawazome,[9] T. Kobuchi,[1] A. Komori,[1] R. Kumazawa,[1]
S. Masuzaki,[1] T. Minami,[1] J. Miyazawa,[1] T. Morisaki,[1] S. Morita,[1] S. Muto,[1] T. Mutoh,[1]
Y. Nagayama,[1] Y. Nakamura,[1] H. Nakanishi,[1] Y. Narushima,[1] K. Nishimura,[1]
N. Noda,[1] T. Notake,[10] H. Nozato,[11] S. Ohdachi,[1] Y. Oka,[1] S. Okajima,[12] M. Osakabe,[1]
T. Ozaki,[1] B. J. Peterson,[1] A. Sagara,[1] T. Saida,[13] K. Saito,[10] S. Sakakibara,[1]
R. Sakamoto,[1] Y. Sakamoto,[5] M. Sasao,[13] K. Sato,[1] M. Sato,[1] T. Seki,[1] M. Shoji,[1]
H. Suzuki,[12] N. Takeuchi,[10] K. Toi,[1] T. Tokuzawa,[1] Y. Torii,[10] K. Tsumori,[1] T. Watari,[1]
H. Yamada,[1] I. Yamada,[1] S. Yamamoto,[10] T. Yamamoto,[10] Y. Yoshimura,[1] K. Itoh,[1]
K. Matsuoka,[1] K. Ohkubo,[1] S. Sudo,[1] T. Uda,[1] K. Yamazaki,[1] and O. Motojima[1]

[1]National Institute for Fusion Sciences, Toki, Gifu 509-5292, Japan
[2]Department of Nuclear Engineering, Kyoto University, Kyoto 606-8501, Japan
[3]Graduate School of Engineering, Hokkaido University, Sapporo 060-8628, Japan
[4]Institute fur Plasmaphysik Forschungszentrum, Julich GmbH 52425, Julich, Germany
[5]Japan Atomic Energy Research Institute, Naka, 311-0193, Japan
[6]Graduate School of Engineering, Osaka University, Suita, Osaka 565-0871, Japan
[7]Department of Fusion Science, School of Mathematical and Physical Science, Graduate University
for Advanced Studies, Hayama, 240-0193, Japan
[8]Research Institute for Applied Mechanics, Kyushu University, Kasuga, 816-8580, Japan
[9]Graduate School of Energy Science, Kyoto University, Uji 611-0011, Japan
[10]Department of Energy Engineering and Science, Nagoya University, 464-8603, Japan
[11]Graduate School of Frontier Sciences, The University of Tokyo 113-0033, Tokyo, Japan
[12]Chubu University, Kasugai, Aichi, 487-8501, Japan
[13]Graduate School of Engineering, Tohoku University, Sendai, 980-8579, Japan

Characteristics of transport in electron internal transport barriers (ITB) and in the vicinity of a rational surface with a magnetic island are studied with transient transport analysis as well as with steady state transport analysis. Associated with the transition of the radial electric field from a small negative value (ion-root) to a large positive value (electron-root), an electron ITB appears in the Large Helical Device [M. Fujiwara *et al.*, Nucl. Fusion **41**, 1355 (2001)], when the heating power of the electron cyclotron heating exceeds a power threshold. Transport analysis shows that both the standard electron thermal diffusivity, χ_e, and the incremental electron thermal diffusivity, χ_e^{inc} (the derivative of normalized heat flux to temperature gradient, equivalent to heat pulse χ_e), are reduced significantly (a factor 5–10) in the ITB. The χ_e^{inc} is much lower than the χ_e by a factor of 3 just after the transition, while χ_e^{inc} is comparable to or even higher than χ_e before the transition, which results in the improvement of electron transport with increasing power in the ITB, in contrast to its degradation outside the ITB. In other experiments without an ITB, a significant reduction (by one order of magnitude) of χ_e^{inc} is observed at the O-point of the magnetic island produced near the plasma edge using error field coils. This observation gives significant insight into the mechanism of transport improvement near the rational surface and implies that the magnetic island serves as a poloidally asymmetric transport barrier. Therefore the radial heat flux near the rational surface is focused at the X-point region, and that may be the mechanism to induce an ITB near a rational surface. © *2004 American Institute of Physics.* [DOI: 10.1063/1.1688787]

I. INTRODUCTION

Recently electron thermal transport barriers have been observed with dominant electron cyclotron heating in plasmas with negative magnetic field shear in many tokamaks.[1–6] In these experiments, the radial profiles of rotational trans-form (safety factor) are measured or calculated and the role of magnetic shear in the formation of the electron internal transport barrier is discussed and the role of radial electric field E_r shear on the electron and ion transport barrier has been studied in tokamak plasma.[7,8] In stellarator plasmas, both the electron and ion ripple losses are sensitive to the radial electric field and electron and ion radial fluxes are functions of the radial electric field in the plasma. Since the

---

2551

electron radial flux is equal to the ion radial flux in the steady state condition, the radial electric field which gives identical ion and electron radial flux is called a "root." The radial electric field with positive (negative) value is called electron (ion) root, because the electron (ion) flux exceeds the ion (electron) flux at zero radial electric field. Because the magnitude of the radial electric field is much larger in the electron root, the reduction of neoclassical transport due to the radial electric field is expected in the electron root rather than the ion root. In contrast to the electron thermal transport barriers in tokamak plasmas, in a stellarator where the magnetic shear is negative, the electron internal transport barrier (ITB) has been observed associated with the transition from ion root (large neoclassical flux with a small E_r) to the electron root (small neoclassical flux with a large positive E_r), when the collisionality becomes low enough for the transition.[9–12] Although the mechanism of ITB formation associated with the transition from ion root to electron root has been studied,[10,11] the quantitative study of the incremental electron thermal diffusivity, $\chi_e^{inc}[=d(Q/n_e)/d(\nabla T_e)]$ has been scarce in ITB plasmas in helical devices in spite of its importance in understanding transport in toroidal devices.[13]

In the L-mode plasma, an instability, such as the electron temperature gradient mode (ETG),[14,15] often results in the sharp increase of the thermal diffusivity above the critical electron temperature gradients and determines the upper limit of the electron temperature for the available heating power.[16] A sharp increase of incremental thermal diffusivity is usually observed near the critical temperature gradient. The temperature dependence of the thermal diffusivity is an extremely important issue for characterizing the ITB and having a prospect for plasma performance with an electron ITB in the high temperature regime required for nuclear fusion. The change of sign of the temperature dependence from positive to negative is required for the transition from L-mode plasma to the ITB plasma. However, the quantitative study for this temperature dependence of thermal diffusivity has not been done. Although the foot point of electron ITB was observed to locate at the $q=2$ surface, where the $m/n=2/1$ magnetic island sometimes appears, in Large Helical Device (LHD) plasmas,[17,18] the role of magnetic islands and rational surfaces on the electron heat transport and the formation of an electron ITB has not been investigated. In this paper, a quantitative study for (1) the electron thermal diffusivity normalized by gyro-Bohm scaling, $\chi_e/(T_e^{3/2}/B^2)$, (2) incremental χ_e, (3) temperature dependence of χ_e is discussed based on the transport analysis with power balance and transient transport analysis using modulated electron cyclotron heating (ECH) and cold pulse propagation. The effect of a magnetic island on the formation of ITB is also discussed.

II. CHARACTERISTICS OF ELECTRON INTERNAL TRANSPORT BARRIER (ITB)

The Large Helical Device (LHD) is a toroidal helical magnetic device (Heliotron device) with a major radius of $R_{ax}=3.5$–4.1 m, an average minor radius of 0.6 m, and a magnetic field B of 0.5–3 T.[19] The radial profiles of E_r are
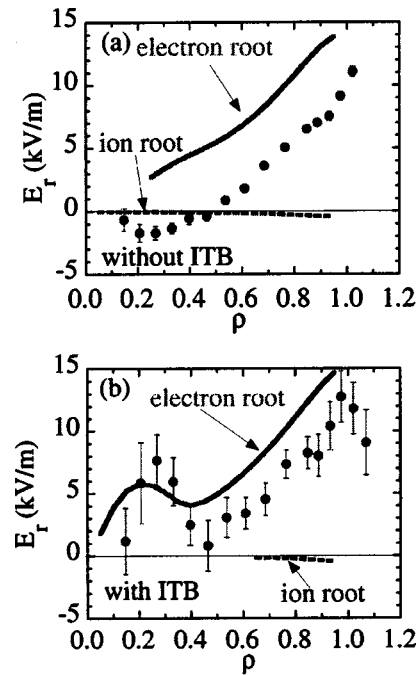

FIG. 1. Radial profiles of radial electric field measured and predicted for the plasma in (a) ion root and (b) electron root with ITB. The closed circles are the radial electric field measured with charge exchange spectroscopy (CXS) and the solid lines are radial electric field calculated using the diffusion coefficient calculation by the Monte Carlo method (DCOM) code.

derived from poloidal flow velocity v_θ measured with charge exchange spectroscopy (CXS) at the midplane in LHD by using a charge exchange reaction between fully ionized neon (0.5%–1%) impurity and atomic hydrogen from the neutral beam.[20] The contribution of the toroidal flow velocity and pressure gradient of neon to the radial electric field are negligibly small (0.3 kV/m and 0.1 kV/m, respectively), because of the damping of toroidal flow and the higher charge of the measured impurity. Three neutral beams with a beam energy of 130–145 keV and an absorbed power of 1.3 MW are injected from 0.3 to 3.3 s to initiate and sustain the plasma and ECH in the second harmonic resonance with a frequency of 82.4 GHz and 84 GHz and with the power of 0.63–0.88 MW is added for $t=1.7$–2.2 s. The focal point of the ECH (Ref. 21) is tuned exactly at the magnetic axis R_{ax} of 3.8 m (major radius in vacuum R_{ax}^v of 3.75 m), which is measured with a soft x-ray CCD camera.[22] The transition from ion root to electron root is observed near the plasma center with localized ECH, when the plasma is well into the collisionless regime ($\nu_b^* < 0.3$) by decreasing the electron density. As seen in Fig. 1, the outer half of the plasma is in the electron root because of the collisionality of the plasma is low enough in this region even without ECH. When the plasma collisionality is low enough ($\nu_b^* = 0.2$ at $\rho = 0.27$) for the transition of ion root to electron root, the formation of an electron internal transport barrier is observed for the plasma with ECH power above the threshold.[17,23] The radial profiles of radial electric field measured are well predicted by the neoclassical (NC) prediction using the diffusion coefficient calculation by the Monte Carlo method (DCOM) code[24,25] as shown in Fig. 1.
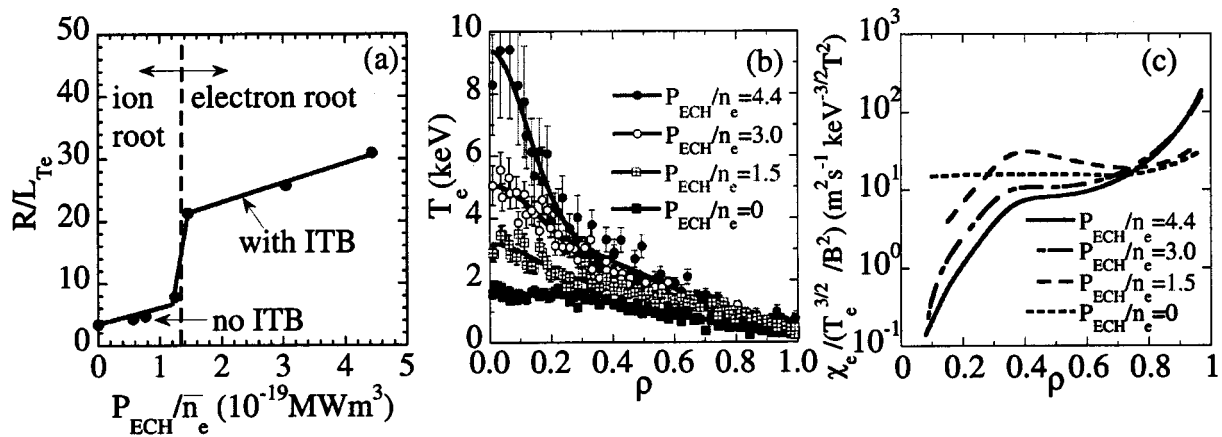
FIG. 2. (a) The peak value of normalized electron temperature gradient R/L_{T_e} inside the ITB region $\rho<0.3$ as a function of ECH power normalized by electron density, P_{ECH}/n_e and radial profiles of (b) electron temperature in LHD (#32940, #32957, #32958 averaged with four time slices) and (c) electron thermal diffusivity normalized by $T_e^{3/2}/B^2$.

A normalized electron temperature gradient R/L_{T_e}, where R is the major radius and L_{T_e} is the scale length of electron temperature gradient, is evaluated for the plasmas with various ECH power normalized by the electron density as seen in Fig. 2(a). There is a clear transition of temperature gradient in the formation of the LHD electron ITB and the transition is associated with the transition from ion root (weak negative radial electric field) to electron root (large positive electric field) in the collisionless regime (ν_b^* <0.3). When the ECH power exceeds the power threshold, the central T_e increases significantly and a large temperature gradient appears near the plasma center at $\rho<0.3$, while there is not much change observed in the profiles of electron density, rotational transform ι and ion temperature. The electron temperature profile becomes more peaked after the formation of the electron ITB and the central electron temperature strongly depends on the ECH power. A smoothed curve with a function of $c_1+c_2\rho^2+c_3\exp(-\rho^2/c_4^2)$, for the transport analysis, where c_1-c_4 are fitting parameters, are also plotted in Fig. 2(b). When the transport in the plasma is gyro-reduced Bohm transport, the thermal diffusivity can be expressed as $\chi_B\rho^*$, where χ_B is the thermal diffusivity in Bohm scaling and ρ^* is a normalized gyro-radius.[26] Therefore the thermal diffusivity is proportional to $T^{3/2}/B^2$ when the transport is dominated by the gyro-reduced Bohm transport. In order to evaluate the improvement of electron transport in the plasma with an electron ITB, the electron thermal diffusivity is normalized by the gyro-reduced Bohm scaling of $T_e^{3/2}/B^2$ as shown in Fig. 2(c). The normalized thermal diffusivity decreased towards the plasma center and reaches low levels close to 0.1 m^2 s^{-1}/(keV$^{3/2}$ T^{-2}) in the LHD electron ITB. This is in contrast to the radial profile of normalized electron thermal diffusivity observed in JT60U, where the minimum normalized thermal diffusivity is located at one-third of the plasma minor radius ($\rho=0.35$).[27,28]

Although there is a significant observed increase of T_e, no increase of ion temperature is observed [Fig. 2(b)], which is in contrast to the formation of both ion and electron transport barrier in ECH-driven ITB plasmas in CHS, where the heating power to ions is comparable to that to electrons be-

cause of the lower energy of NBI (30–40 keV).[29] No increase of ion temperature in LHD may be because the growth rate of the long wavelength turbulence contributing the ion heat transport is enhanced due to the increase of the ratio of T_e/T_i. (The degradation of ion transport associated with the increase of T_e/T_i ratio are often observed.[30–32])

III. INCREMENTAL ELECTRON THERMAL DIFFUSIVITY INSIDE THE ITB

The formation of the electron internal transport barrier is due to the bifurcation phenomena of the electron heat transport, which is clearly demonstrated in the relation between the electron heat flux normalized by density and temperature gradient as seen in Fig. 3(a). At the transition from an L-mode plasma to the ITB plasma, the T_e gradient near the plasma center ($\rho=0.15$) jumps from 3.6 keV/m to 13 keV/m even for the same magnitude of heat flux (reduction of χ_e by a factor of 4). After the transition to an ITB plasma, χ_e decreases up to 3 m^2/s (reduction of χ_e by a factor of 8). The incremental thermal diffusivity, χ_e^{inc}, in the ITB plasma near the plasma center ($\rho=0.15$), is 1 m^2/s, which is lower than that for the plasma without ITB by a factor of 20. The incremental thermal diffusivity is also estimated from the time lag of the heat pulses, which is given from the phase delay between the Fourier transforms of δT_e and of the modulated ECH power. The incremental heat diffusivity is given by the propagation velocity of the heat pulse (the slope of time lag to minor radius of the plasma).[33] The heat diffusivity in the ITB plasma decreases by a factor of 5 compared to that in the no-ITB plasma (without base ECH) and it is much smaller than that outside the ITB (see the data of off-axis MECH experiment) by one order of magnitude as seen in Fig. 3(b), which is consistent with the results from power balance.

Another approach to estimate the incremental electron thermal diffusivity is cold pulse propagation induced by a tracer encapsulated solid pellet (TESPEL) (Ref. 34) ablated near the plasma edge. The thermal diffusivity can be derived with transient transport analysis using the perturbed heat transport equation written as
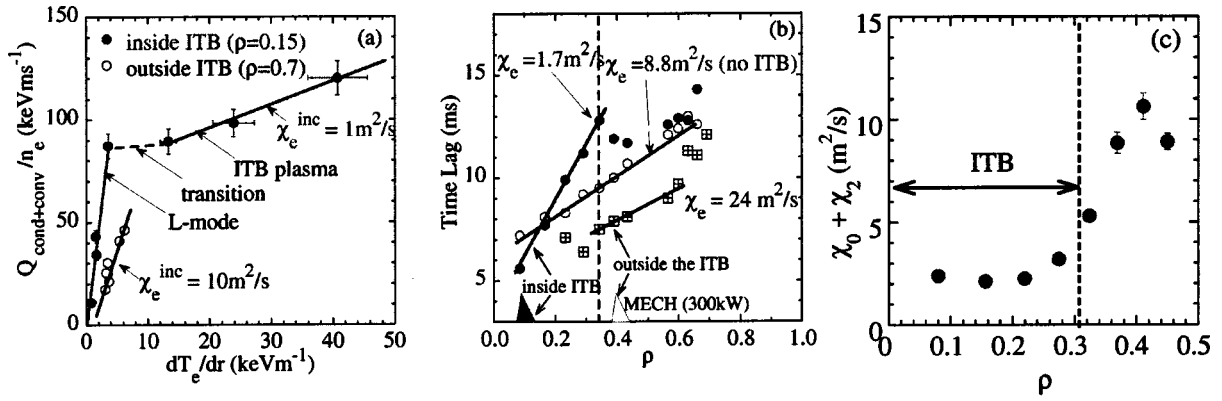
FIG. 3. (a) Electron heat flux nomalized by electron density as a function of the electron temperature gradient and the radial profile of (b) the time lag of the heat propagation in the plasma with 300 kW modulated electron cyclotron heating (MECH) with a frequency of 20 Hz and (c) electron thermal diffusivity derived from the cold pulse propagation. The triangles in (b) represent the location of the deposition peak of ECH.

$$\frac{3}{2}n_e\frac{\partial\delta T_e}{\partial t}=\nabla\cdot\left(n_e(\chi_0+\chi_2)\nabla\delta T_e-n_e\chi_1\frac{-\nabla T_e}{T_e}\delta T_e\right),$$
(1)

$$\chi_0(r)=-\frac{Q_e}{n_e\nabla T_e},$$
(2)

$$\chi_1(r)=\frac{\partial\chi_e}{\partial T_e}T_e,$$
(3)

$$\chi_2(r)=\frac{\partial\chi_e}{\partial\nabla T_e}\nabla T_e.$$
(4)

When the normalized heat flux perturbation, y, and the normalized perturbation gradient, x, are defined as

$$y(r,t)=\frac{1}{rn_e\delta T_e}\int_0^r\frac{3}{2}n_e\frac{\partial\delta T_e}{\partial t}udu,$$
(5)

$$x(r,t)=\frac{\nabla\delta T_e}{\delta T_e}.$$
(6)

Equation (1) can be written as $y(r,t)=a(r)x(r,t)-b(r)$, $a=\chi_0+\chi_2$, $b=\chi_1(-\nabla T_e/T_e)$, here r is the averaged minor radius. The coefficients $a(r)$ and $b(r)$ are derived by fitting the $x(r,t)$ and $y(r,t)$ with a line. Figure 3(c) shows the radial profiles of thermal diffusivity $a=\chi_0+\chi_2$. The cold pulse propagation experiment also shows the significant reduction of electron thermal diffusivity inside the ITB ($2\ m^2/s$ inside and $10\ m^2/s$ outside the ITB). The time resolution of the measurement of ion temperature is poor and not fast enough to study the cold pulse in the ion temperature and no information for the cold pulse in ion temperature is obtained. Since there is no increase of ion temperature observed associated with the formation of the electron internal transport barrier, the reduction of ion thermal diffusivity is not expected.

IV. TEMPERATURE DEPENDENCE OF ELECTRON THERMAL DIFFUSIVITY

The temperature dependence of thermal diffusivity $\alpha=(T_e/\chi_e)(d\chi_e/dT_e)$ is an important parameter to study the plasma with ITB. In the L-mode, the parameter α is positive

and typically it is 1.5, which is predicted from the gyro-reduced Bohm scaling and is also consistent with the power degradation of the global energy confinement in LHD of $\tau_E\propto(P/n)^{-0.6}$.[35] If the parameter α stays positive, the formation of an ITB would never occur, because spontaneous increase of electron temperature during the formation of an ITB requires a negative α. Therefore α would be the most reasonable parameter to confirm whether the plasma is in the L-mode regime or the ITB regime, especially near the boundary between the L-mode and ITB mode in space and in time, and therefore negative α can be a definition of an ITB plasma. The transient transport analysis with a cold pulse indicates the existence of χ_1 due to the strong temperature dependence of electron thermal diffusivity. The temperature dependence is investigated by power balance analysis and the cold pulse experiment. When the electron thermal diffusivity is proportional to the temperature to the power of α as T_e^α, α can be derived from χ_1 as $\alpha=\chi_1/\chi_e$.

As shown in Fig. 4, the temperature dependence parameter in the core region is even worse ($\alpha=2.7$) than that near the plasma edge before the transition to ITB. However, it changes its sign from positive to negative (from 2.7 to -1.5) associated with the formation of an ITB. Outside the ITB region, the positive temperature dependence of electron thermal diffusivity ($\alpha=1.6$) is observed, which is consistent with the temperature dependence ($\alpha=1.5$) of the gyro-reduced Bohm transport. The change of sign of the temperature dependence of the electron thermal diffusivity is a key to the formation of the ITB. This negative temperature dependence of thermal diffusivity $\alpha<0$, is also consistent with the significant reduction of χ_e^{inc} below χ_e inside the ITB as seen in Fig. 3(a), because when $\chi_e^{inc}<\chi_e$ inside the ITB, the χ_e decreases as the electron temperature is increased with the increase of normalized heat flux.

It should be noted that the change of sign of α from positive to negative is a key to electron ITB formation. If the α remains positive there should be no increase of electron temperature after the onset of electron ITB formation, because the radial heat flux tends to decrease after the ITB formation. The temperature gradient dependence parameter of thermal diffusivity $\beta[=(\nabla T_e/\chi_e)(d\chi_e/d\nabla T_e)]$ is differ-
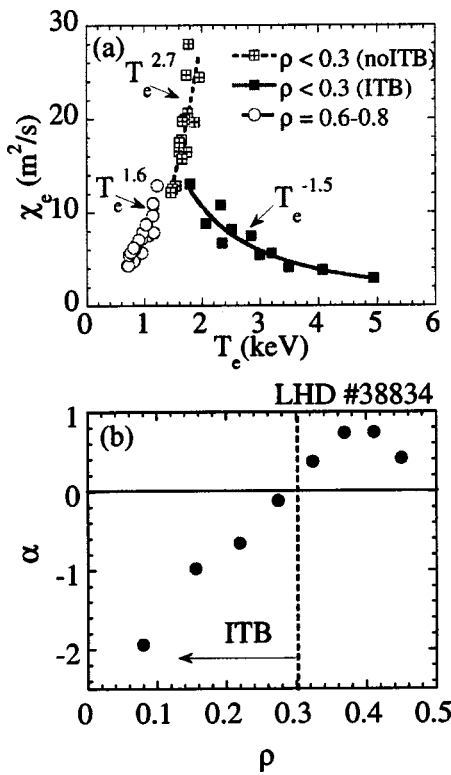
FIG. 4. (a) Electron thermal diffusivity as a function of electron temperature and (b) radial profile of the temperature dependence derived from the cold pulse propagation experiment.
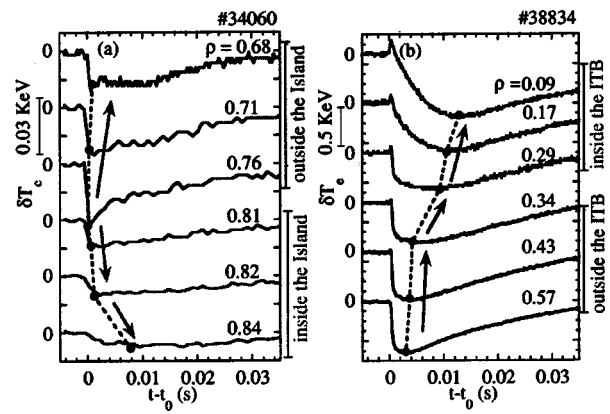

FIG. 5. (a) Time evolution of electron temperature measured with ECE in the plasma with a cold pulse experiment near the (a) 1/1 magnetic island and (b) the 1/2 magnetic island.

ent from α because of the peaking of electron temperature profile after the ITB formation. The beta values inside the electron ITB are in the range of -0.4 to -0.7 and stay above -1, where an unstable situation occurs. As shown in Fig. 4(b), the temperature dependence parameter, α, derived from the cold pulse propagation with transient transport analysis also shows the same trend. The temperature dependence is positive ($\alpha=0.5-1.0$) outside the ITB, while it becomes negative inside the ITB and decreases up to -2 towards the magnetic axis.

V. TRANSPORT NEAR THE RATIONAL SURFACE

It is widely observed that the foot point of the ITB is related to the rational surface ($q=2$ surface) both in tokamak and helical plasmas. In LHD, the radial profiles of electron temperature strongly depends on the radial profile of the rotational transform controlled by the toroidal plasma current driven by a neutral beam.[18] When the rational surface is located near the plasma axis ($\rho=0.3$), the foot point is located at the $q=2$ surface, while there is no clear foot point observed when there is no $q=2$ surface inside the plasma. These observation suggests the importance of the rational surface for the formation of an ITB. In order to study the role of the rational surface and why a magnetic island often appears at the rational surface, the heat transport near the magnetic island is investigated using cold pulse propagation. Figure 5 shows the time evolution of the cold pulse, near the 1/1 magnetic island and the 1/2 magnetic island. The cold pulse is produced at $\rho=0.75$ by injecting the TESPEL to the

X-point of the magnetic island.[36] The cold pulse propagation starts at the boundary of the magnetic island (O-point) and the cold pulse propagates both toward the plasma center (outside of magnetic island) and towards the plasma edge (inside the magnetic island). The details of the topology of the magnetic island and of the TESPEL injection and ECE measurements are described in a previous paper.[37] It should be noted that this magnetic island is a stationary island and does not rotate, which makes this experiments technically much easier than the case when the magnetic island is rotating as in tokamak plasmas. The propagation inside the magnetic island is much slower than that outside the magnetic island, which indicates that the thermal diffusivity inside the magnetic island is significantly reduced. The cold pulse is degraded when the pulse reaches the ITB as shown in Fig. 5(b). The cold pulse propagates much slower inside the ITB than that outside the ITB, which indicates the lower thermal diffusivity inside the ITB. It should be noted that Fig. 5(a) shows the cold pulse propagation from the boundary to the center of O-point of magnetic island, Fig. 5(b) shows the cold pulse propagation across the magnetic island, which is located at the foot point of the ITB ($\rho=0.3$).

Figure 6 shows time delay, which is defined as the time differences between the time of TESPEL injection and the peak of the pulse and indicated with closed circles in Fig. 5. The size of the 1/1 magnetic island in Fig. 6(a) is evaluated from the temperature profiles measured with ECE. On the other hand, the size of the 1/2 magnetic island in Fig. 6(b) is too small to be measured, because the ECE measurement locates near the X-point of the magnetic island. Therefore the size of the 1/2 magnetic island is estimated from the electron temperature profile near the O-point of magnetic island measured with YAG Thomson scattering using mapping of flux surfaces. The time evolution of the electron temperature after the pellet injection is well reproduced by the diffusive model in the slab model. This is because the increase of density due to the TESPEL is small enough not to enhance the turbulence and change the transport which is in contrast to the experiment in Wendelstein VII-AS where a large pellet triggers MHD oscillations.[38] However, the absolute value of the thermal diffusivity estimated here is uncertain due to the simplic-
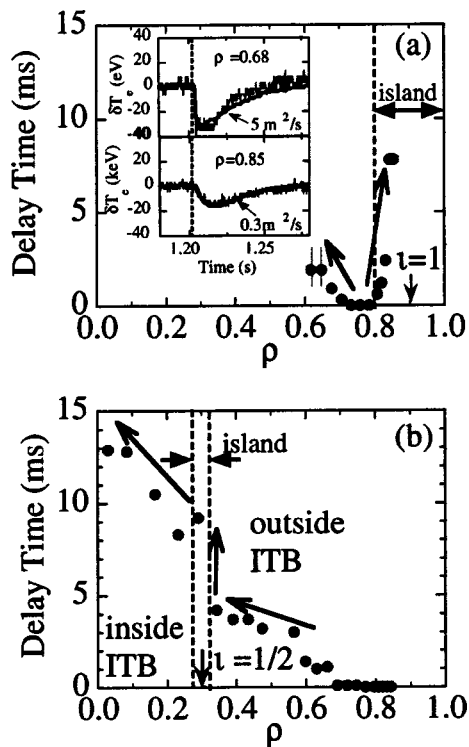
FIG. 6. (a) Radial profiles of time to peak of cold pulse propagation near the (a) O-point of the 1/1 magnetic island and (b) X-point of the 1/2 magnetic island.
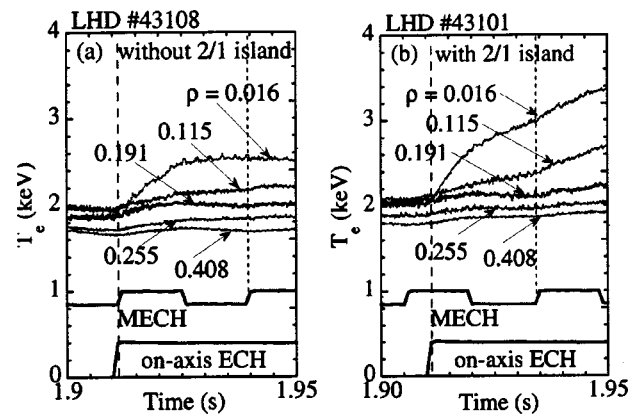

FIG. 7. (a) Time evolution of the electron temperature measured with ECE at various radii for the plasma (a) without a 2/1 island and (b) with a 2/1 island.

ity of the model used for the analysis, because the structure of the magnetic island (the effect of the poloidal asymmetry) is not included in the analysis. The thermal diffusivity for the best fit to the experimental data is $0.3 \, \text{m}^2/\text{s}$ (with an uncertainty of factor of 2) inside the magnetic island and $5.0 \, \text{m}^2/\text{s}$ (with an uncertainty of factor of 4) outside of the magnetic island. There are jumps in the delay time at the boundary of magnetic island or near the rational surface [$i = 1$ in Fig. 6(a) and $i = 1/2$ in Fig. 6(b)]. This jump of time delay suggests the reduction of transport near the rational surface or at the boundary of the magnetic island.

The sheared poloidal flows and sheared radial electric field are observed at the boundaries of the magnetic island in LHD when the $n/m = 1/1$ magnetic island is produced by external perturbation coils, because the poloidal flow vanishes inside the static magnetic island.[39] The E_r shear and the shearing rate given by the measurements is more than $0.2–0.4 \, \text{MV/m}^2$ and $10^5 \, \text{s}^{-1}$ at the boundary of the magnetic island, which is comparable to the threshold value of dE_r/dr in a Heliotron configuration.[40] Even when there is no current in the external perturbation coil, there are intrinsic magnetic islands at the $q = 1$ and/or $q = 2$ rational surfaces due to the error field depending on the plasma parameters[41,42] and this magnetic island does not rotate in contrast to the magnetic island driven by a tearing mode in a tokamak. Therefore the sheared radial electric field is expected to exist in the intrinsic magnetic island as well as in the magnetic island produced by an external coil current. One of the candidates of significant reduction of transport near the rational surface is

the radial electric field shear which appears at the boundary of the magnetic island.

The electron heat transport is improved at the boundary of the magnetic island as well as inside the magnetic island and the magnetic island serves as a poloidally asymmetric transport barrier. Therefore the radial heat flux near the magnetic island is focused at the X-point region, and that may be the mechanism to induce an ITB near a magnetic island at a rational surface. The ITB plasma can be achieved without rational surfaces or a magnetic island. However, the ITB formation becomes easier (with lower ECH power) when there is a magnetic island in the plasma. In order to study the effect of a magnetic island on the formation of an ITB, external field coils are applied to control the size of the magnetic island.

Figure 7 shows the time evolution of the electron temperature for the various plasma radii at the formation of the ITB. When the external field is applied, which cancels the natural 2/1 island usually appears at the $i = 1/2$ rational surface, the electron temperature increases after the onset of on-axis ECH and saturates within 15 ms, which is comparable to the energy confinement time of the plasma without an ITB. However when there is no canceling external magnetic field applied, the electron temperature keeps increasing over 100 ms after the onset of ECH and reaches 4 keV, which indicates the significant improvement of heat transport in the plasma with the ITB. This experiment demonstrates that the 2/1 magnetic island contributes to the formation of the ITB (reduces the power threshold for the transition to the ITB) and supports the hypothesis that the radial heat flux near the rational surface is focused at the X-point region when the magnetic island appears in the plasma. Since the flattening of the electron temperature inside the magnetic island itself even decreases the total stored kinetic energy, the magnetic island does not contribute to the increase of plasma stored energy for the plasma when there is no ITB. It should be noted that although the magnetic island contributes to the formation of the ITB, it does not contribute the improvement of transport in the ITB plasmas. (A high performance ITB plasma can be achieved without a magnetic island when there is enough heating power.) Although the foot

point of the ITB is located at the $i = 1/2$ rational surface when there is the 2/1 magnetic island, the foot point moves towards the plasma center and is not located at the $i = 1/2$ rational surface when the 2/1 magnetic island disappears by the canceling field.

VI. CONCLUSIONS

In conclusion, a clear transition phenomena in the electron heat flux is observed associated with the transition from the ion root to the electron root in the LHD plasmas. The normalized thermal diffusivity decreased towards the plasma center and reaches low levels close to $0.1 \, \mathrm{m^2 \, s^{-1}}/(\mathrm{keV^{3/2} \, T^{-2}})$ in the LHD electron ITB, which is much lower than that without an ITB by two orders of magnitude. The significant reduction of the incremental thermal diffusivity, χ_e^{inc}, by one order of magnitude is observed inside the ITB with the power balance analysis and transient transport of analysis by heat pulse propagation with modulated ECH and cold pulse propagation by TESPEL injection. The temperature dependence of the thermal diffusivity, α, is evaluated from power balance χ_e and temperature dependent term χ_1 derived from cold pulse propagation. It is positive in the L-mode plasma ($\alpha = 1 - 3$) and becomes negative ($\alpha = -1$ to -2) inside the ITB. Since the heat transport is improved inside the magnetic island and the radial electric field shear is produced at the boundary of the magnetic island, the magnetic island located near the foot point of the ITB contributes to the formation of the ITB by reducing the threshold power.

ACKNOWLEDGMENTS

[1] T. Fujita, S. Ide, H. Shirai, M. Kikuchi, O. Naito, Y. Koide, S. Takeji, H. Kubo, and S. Ishida, Phys. Rev. Lett. **78**, 2377 (1997).
[2] M. R. deBaar, G. M. D. Hogeweij, N. J. Lopes Cardozo, A. A. M. Oomens, and F. C. Schuller, Phys. Rev. Lett. **78**, 4573 (1997).
[3] P. Buratti, E. Barbato, G. Bracco et al., Phys. Rev. Lett. **82**, 560 (1999).
[4] S. Gunter, R. C. Wolf, F. Leuterer et al., Phys. Rev. Lett. **84**, 3097 (2000).
[5] Z. A. Pietrzyk, C. Angioni, R. Behn, S. Coda, T. P. Goodman, M. A. Henderson, F. Hofmann, and O. Sauter, Phys. Rev. Lett. **86**, 1530 (2001).
[6] C. D. Challis, Yu. F. Baranov, G. D. Conway et al., Plasma Phys. Controlled Fusion **43**, 861 (2001).
[7] B. W. Stallard, C. M. Greenfield, G. M. Staebler et al., Phys. Plasmas **6**, 1978 (1999).
[8] L. L. Lao, K. H. Burrell, T. S. Casper et al., Phys. Plasmas **3**, 1951 (1996).
[9] H. Idei, K. Ida, H. Sanuki et al., Phys. Rev. Lett. **71**, 2220 (1993).
[10] A. Fujisawa, H. Iguchi, T. Minami et al., Phys. Rev. Lett. **82**, 2669 (1999).
[11] U. Stroth, K. Itoh, S.-I. Itoh, H. Hartfuss, and H. Laqua, Phys. Rev. Lett. **86**, 5910 (2001).
[12] K. Ida, H. Funaba, S. Kado et al., Phys. Rev. Lett. **86**, 5297 (2001).
[13] F. Wagner and U. Stroth, Plasma Phys. Controlled Fusion **35**, 1321 (1993).
[14] W. Dorland, F. Jenko, M. Kotschenreuther, and B. N. Rogers, Phys. Rev. Lett. **85**, 5579 (2000).
[15] J. Q. Dong, H. Sanuki, K. Itoh, and L. Chen, Phys. Plasmas **9**, 4699 (2002).
[16] F. Ryter, C. Angioni, M. Beurskens et al., Plasma Phys. Controlled Fusion **43**, A323 (2001).
[17] T. Shimozuma, S. Kubo, H. Idei et al., Plasma Phys. Controlled Fusion **45**, 1183 (2003).
[18] Y. Takeiri, T. Shimozuma, S. Kubo et al., Phys. Plasmas **10**, 1788 (2003).
[19] M. Fujiwara, K. Kawahata, N. Ohyabu et al., Nucl. Fusion **41**, 1355 (2001).
[20] K. Ida, S. Kado, and Y. Liang, Rev. Sci. Instrum. **71**, 2360 (2000).
[21] S. Kubo, T. Shimozuma, H. Idei et al., J. Plasma Fusion Res. **78**, 99 (2002).
[22] Y. Liang, K. Ida, S. Kado et al., Plasma Phys. Controlled Fusion **44**, 1383 (2002).
[23] K. Ida, T. Shimozuma, H. Funaba et al., Phys. Rev. Lett. **91**, 085003 (2003).
[24] A. Wakasa, S. Murakami, H. Maassberg, C. D. Beidler, N. Nakajima, K. Y. Watanabe, H. Yamada, M. Okamoto, S. Oikawa, and M. Itagaki, J. Plasma Fusion Res. SERIES **4**, 408 (2001).
[25] S. Murakami, U. Gasparino, H. Idei, S. Kubo, H. Maassberg, N. Marushchenko, N. Nakajima, M. Rome, and M. Okamoto, Nucl. Fusion **40**, 693 (2000).
[26] H. Yamada, K. Y. Watanabe, K. Yamazaki et al., Nucl. Fusion **41**, 901 (2001).
[27] T. Fujita, T. Fukuda, Y. Sakamoto et al., "Formation conditions of electron internal transport barriers in JT-60U plasmas," Plasma Phys. Controlled Fusion (to be published).
[28] K. Ida, T. Fujita, T. Fukuda et al., "Comparison of electron internal transport barrier in the Large Helical Device and JT-60U plasmas," Plasma Phys. Controlled Fusion (to be published).
[29] T. Minami, A. Fujisawa, H. Iguchi et al., Nucl. Fusion **44**, 342 (2004).
[30] C. C. Petty, M. R. Wade, J. E. Kinsey, R. J. Groebner, T. C. Luce, and G. M. Staebler, Phys. Rev. Lett. **83**, 3661 (1999).
[31] S. Ide, T. Suzuki, Y. Sakamoto, H. Takenaga, Y. Koide, T. Fujita, T. Fukuda, Y. Kamada, H. Shirai, and T. Takizuka, Plasma Phys. Controlled Fusion **44**, A137 (2002).
[32] K. Ida, K. Kondo, K. Nagasaki et al., Plasma Phys. Controlled Fusion **40**, 793 (1998).
[33] S. Inagaki, K. Ida, N. Tamura, T. Shimozuma, S. Kubo, Y. Nagayama, K. Kawahata, S. Sudo, and K. Ohkubo, "Cold pulse experiments in plasma with an electron internal transport barrier on LHD," Plasma Phys. Controlled Fusion (to be published).
[34] S. Sudo, N. Tamura, K. Khlopenkov et al., Plasma Phys. Controlled Fusion **44**, 129 (2002).
[35] H. Yamada, K. Y. Watanabe, S. Sakakibara et al., Phys. Rev. Lett. **84**, 1216 (2000).
[36] S. Inagaki, N. Tamura, K. Ida, Y. Nagayama, K. Kawahata, S. Sudo, T. Morisaki, K. Tanaka, and T. Tokuzawa, Phys. Rev. Lett. **92**, 055002 (2004).
[37] K. Ida, S. Inagaki, N. Tamura et al., Nucl. Fusion **44**, 290 (2004).
[38] J. Lyon, Proceedings of the 24th EPS Conference, Berchtesgaden, 1997, Vol. 21A, p. 1629.
[39] K. Ida, N. Ohyabu, T. Morisaki et al., Phys. Rev. Lett. **88**, 015002 (2002).
[40] K. Itoh, S.-I. Itoh, A. Fukuyama, H. Sanuki, and M. Yagi, Plasma Phys. Controlled Fusion **36**, 123 (1994).
[41] K. Narihara, K. Y. Watanabe, I. Yamada et al., Phys. Rev. Lett. **87**, 135002 (2001).
[42] N. Ohyabu, K. Ida, T. Morisaki et al., Phys. Rev. Lett. **88**, 055005 (2002).